Am J Transl Res 2016;8(8):3460-3470
www.ajtr.org /ISSN:1943-8141/AJTR0032486

*Original Article*

# Peroxisome proliferator-activated receptor-γ agonist troglitazone suppresses transforming growth factor-β1 signalling through miR-92b upregulation-inhibited Axl expression in human keloid fibroblasts *in vitro*

Hua-Yu Zhu[1*], Wen-Dong Bai[2*], Jun Li[1*], Ke Tao[1], Hong-Tao Wang[1], Xue-Kang Yang[1], Jia-Qi Liu[1], Yun-Chuan Wang[1], Ting He[1], Song-Tao Xie[1#], Da-Hai Hu[1#]

*[1]Department of Burns and Cutaneous Surgery, Xijing Hospital, Fourth Military Medical University, Xi'an 710032, Shaanxi, China; [2]Department of Hematology, Urumqi General Hospital of Chinese People's Liberation Army, Urumqi, Xinjiang, China. [*]Equal contributors. [#]Equal contributors.*

Received May 19, 2016; Accepted August 8, 2016; Epub August 15, 2016; Published August 30, 2016

**Abstract:** Keloid, a skin benign tumor, is characterized by overgrowth of fibroblasts and the excessive deposition of extracellular matrix in wounded skin. Peroxisome proliferator-activated receptor-γ (PPAR-γ) agonist was recently evaluated to inhibit fibrosis. This study explored the underlying mechanisms. Fibroblasts isolated from 25 keloid patients (KFs) and fibroblasts isolated from healthy controls (NSFBs) were also subjected to treatment with PPAR-γ agonist troglitazone and antagonist GW9662 or for transfection with miR-92 mimics or inhibitor, Axl siRNA, and miR-92b or Axl promoter constructs, as well as being subjected to qRT-PCR, ELISA, Western blot, protein array, luciferase, and ChIP assays. The data demonstrated that TGF-β1 and Axl proteins were significantly elevated in samples from keloid patients, while troglitazone treatment significantly reduced levels of TGF-β1 and Axl mRNA and proteins in KFs. Moreover, knockdown of Axl expression reduced expression of TGF-β1 and its pathway genes (such as α-SMA and Snail). PPAR-γ regulation of Axl expression was through transcriptional activation of miR-92b. miR-92b expression downregulated Axl expression at both mRNA and protein levels, whereas GW9662 completely reversed the inhibitory effects of miR-92b mimics on Axl expression. Gene ontology analysis of miR-92b targeting genes showed that TGF-β and Axl were both potential targets of miR-92b, as confirmed by luciferase assay. These findings demonstrated that PPAR-γ-induced miR-92b expression inhibited Axl expression and in turn reduced expression of TGF-β1 and the downstream genes in KFs, suggesting that targeting of this novel gene pathway may be useful for therapeutic control of fibrosis or keloid.

**Keywords:** Benign tumor, miR-92b, TGF-β signaling, keloid, Axl, PPAR-γ

## Introduction

Keloid is a benign tumor caused by abnormal wound healing after skin injury [1, 2]. Clinically, keloid is characterized by the overgrowth of fibroblasts and the excessive deposition of the extracellular matrix in injured skin to form unwanted scarring, but the precise process and mechanism are unclear [3]. The most frequently involved sites are the chest, shoulders, head-neck areas, ear lobes, arms, and the upper back [4]. In predisposed individuals, keloid results from abnormal skin repair after skin injury, affecting them cosmetically and functionally. Although it is known that injury to the skin is required for keloid formation, few other risk factors have been recognized. For example, peroxisome proliferator-activated receptor-γ (PPAR-γ) agonist was recently determined to inhibit this abnormal fibrosis formation. Thus, numerous synthetic PPAR-γ activators have been synthesized and identified, such as rosiglitazone, pioglitazone, or troglitazone [5]. PPAR-γ is a nuclear receptor, belonging to the steroid hormone nuclear receptor family. Functionally, PPAR-γ forms a heterodimer with retinoid X receptor-α (RXR-α) and then binds to peroxisome proliferator hormone response elements (PPREs) on the DNA of target genes; this ligand-activated PPAR-γ protein in turn regulates a variety of functions, such as embryo development, cell growth, differentiation, and

lipid metabolism [6]. Altered PPAR-γ expression was also associated with tumorigenesis [7]. PPAR-γ agonist Thiazolidinedione was explored as an insulin-sensitizer in treatment of type 2 diabetes mellitus [8]. In animal experiments, PPAR agonists were shown to control of a variety of neoplasms, including urinary bladder cancer, hemangiosarcoma, liposarcoma/fibrosarcoma, and liver cancer [9, 10], while PPAR-γ agonist Efatutazone was demonstrated to have an acceptable safety profile in control of anaplastic thyroid cancer and metastatic colorectal cancer during Phase I clinical trials [11, 12]. Interestingly, many studies have shown that PPAR-γ possesses an anti-fibrotic effect in the kidney [13], liver [14], pancreas [15], and lung [16], suggesting PPAR-γ agonist may be a promising agent for the control of fibrotic diseases [17]. However, the precise targets and mechanisms of PPAR-γ agonist anti-fibrosis action in keloid fibroblasts remain to be determined, in spite of our growing understanding of the molecular basis for PPAR-γ agonist anti-fibrotic function.

As we know, transforming growth factor (TGF-β) is a pleiotropic cytokine, expressed and secreted by a variety of cells in human body. Altered TGF-β has been associated with many fibrosis-related diseases [18, 19] and accumulating evidence supports the notion that TGF-β is an important pathological factor in excessive scar formation in abnormal wound healing and fibrosis [20]. The therapeutic strategy of targeting TGF-β1 has been reported to control excessive keloid fibrosis [21], while PPAR-γ agonist troglitazone was found to suppress TGF-β1 expression in human dermal fibroblasts, indicating that PPAR-γ agonist possesses therapeutic potential in the treatment of dermal fibrosis (hypertrophic scar or keloid) [22]. Thus, in this study, we investigated the mechanism by which PPAR-γ agonist regulates TGF-β signaling in the inhibition of fibrosis in fibroblasts isolated from keloid patients (KFs). We expected to provide support for troglitazone-inhibited TGF-β1 secretion and signaling in the suppression of fibrosis through troglitazone-upregulated miR-92b to target Axl and TGF-β1 expression in KFs.

## Materials and methods

### *Fibroblasts and culture*

Human primary KFs and normal skin fibroblast (NSFBs) were isolated from surgically excised tissues of 25 keloid patients and healthy controls, cultured as described previously [17]. In this study, the third to the fourth passages of KFs were used in all experiments and cultured in Dulbecco's modified Eagle's medium (DMEM), containing 10% fetal bovine serum (FBS) in a humidified incubator with 5% $CO_2$ at 37°C. For drug treatment, troglitazone (Abcam, Cambridge, MA, USA) was dissolved in dimethyl sulfoxide (DMSO) and diluted in the culture medium and then added to cell culture at a 30 $mmol^{-1}$ dose for 72 h; to the control culture was added an equal amount of DMSO. Furthermore, we also determined whether the effects of troglitazone on KFs are PPAR-γ-dependent by co-incubation of KFs with 1 μM PPAR-γ antagonist GW9662 (Abcam) for 48 h, according to a previous study [22, 23].

### *Main reagents*

Antibodies used for Western blotting analyses included anti-TGF-β1 (ab64715, Abcam), anti-Axl (ab37861, Abcam), anti-α-SMA (ab5694, Abcam), anti-Snail (ab53519, Abcam), and anti-β-actin (ab8224, Abcam) antibodies, while antibodies used for chromatin immunoprecipitation (ChIP) were anti-PPAR-γ (ab45036, Abcam). Axl siRNA reagents were designed using ONTARGET plus SMARTpool against human Axl (siAxl; NM_001699) with sequences of 5'-AAACUUUCCUCAGAAGUUGUUTT-3' and 5'-CAACUUCUGAGGAAAGUUUGGTT-3', while scrambled siRNA was used as a control, with sequences of 5'-AAACUUUCCUCAGAAGUUGUUTT-3' and 5'-CAACUUCUGAGGAAAGUUUGGTT-3'. Moreover, the FAM-modified 2'-OMe oligonucleotides were chemically synthesized and purified with high-performance liquid chromatography by GenePharma (Shanghai, China). 2'-O-me-miR mimics, inhibitor and control were composed of RNA duplexes with the following sequences: miR-92b mimics, 5'-UAUUGCACUCGUCCCGGCCUCC-3'; miR-92b inhibitor, 5'-GGAGGCCGGGACGAGUGCAAUA-3'; scramble oligonucleotide as a negative control, 5'-CAGUACUUUUGUGUAGUACAA-3'.

### *Plasmid construction and transfection*

A potential PPRE (with a DNA core motif of 5'-AGGTCA-3') localized at -1148 to -1142 bp of the transcription start site of the miR-92b promoter, according to a previous study [24]. We amplified this wild type miR-92b promoter, containing PPRE (5'-CACAAGGTCAGGGG-3'), into a

pTransluc vector (Panomics, Redwood City, CA, USA) using PCR with primers (5'-CGGCTGGGAGCTTTAGG-3' and 5'-GCAATATTGGCGGGGGAA-3'). The miR-92b deletion mutant was then generated by deleting 13 bp spanning in the PPRE site with primers of 5'-ATCCACTCGCCTCGGCCTT-3' or 5'-TTCAAGACCAGCCTGGCCAA-3') and subcloned into pTransluc. After DNA sequencing confirmation, these vectors were named PPRE-wt and PPRE-del, respectively.

Moreover, the Axl 3'-UTR cDNA and a mutant with replaced nucleotides in the putative binding site corresponding to the seed-sequence of miR-92b were amplified from 3sp cDNA with primers according to a previous study [25, 26] and ligated into the pGL3 vector (Promega, Madison, WI, USA). The primers for wild type (wt) were 5'-CGGCTGGGAGCTTTAGG-3' and 5'-GCAATATTGGCGGGGGAA-3' and for mutant (mut) were 5'-ATCCACTCGCCTCGGCCTT-3' and 5'-TTCAAGACCAGCCTGGCCAA-3'. These vectors were then used to transfect into the cultured fibroblasts.

For siRNA transfection, KFs were grown and transfected with 25 nM siAxl, or siCtrl using Lipofectamine RNAiMAX transfection reagent (Invitrogen, Carlsbad, CA, USA), according to the manufacturer's protocol. For miRNA, synthetic miR-92b mimics, miR-92b inhibitor or negative controls were transfected into the KFs and examined at varying concentrations (25 nM) using HiPerfect Transfection Reagent (Qiagen, Valencia, CA, USA) following the manufacturer's instructions. 24 h later troglitazone or GW9662 was then added into cell culture for 72 or 48 h.

*Quantitative reverse transcription-PCR (qRT-PCR)*

Fibroblasts were plated in 6-well plates at a density of $3 \times 10^5$ cells/well and cultured overnight. Next, fibroblasts were subjected to gene transfection, troglitazone or GW9662 treatment. At the end of each experiment, total cellular RNA was isolated using TRIzol reagent and the Pure Link RNA mini kit (Invitrogen) and subsequently reverse transcribed into cDNA using an RT kit from Invitrogen, according to the manufacturer's instructions. The resulting cDNA samples were subjected to qPCR amplification using the following primers. Axl primer sequences were 5'-GTGGGCAACCCAGGGAATATC-3' 5'GTACTGTCCCGTGTCGGAAAG-3'; TGF-β1 primers were 5'-GGCCAGATCCTGTCCAAGC-3' and 5'-GTGGGTTTCCACCATTAGCAC-3'; and GAPDH primers were 5'-GGAGCGAGATCCCTCCAAAAT-3' and 5'-GGCTGTTGTCATACTTCTCATGG-3'; miR-92b primers were 5'-TATTGCACTCGTCCCGGCCTCC-3' and a miRNA universal primer (Qiagen, Hilden, Germany); U6-snRNA primers were RNU6B_2 miScript Primer and a miRNA universal primer from Qiagen. qRT-PCR was performed in triplicate on CFX96 Real Time PCR Detection System (Bio-Rad, Hercules, CA, USA). The relative expression level of each transcript was measured using the comparative $C_t$ method and compared to internal controls (GAPDH or U6). All experiments were in triplicate and repeated three times.

*Luciferase reporter assay*

Fibroblasts were seeded into 48-well plates and cultured in 250 μl DMEM supplemented with 10% FBS, and, when reaching to 80-90% confluency, these cells were co-transfected with 400 ng WT-Axl-UTR or mut Axl-UTR plasmid and 20 ng of the control pRL-TK vector carrying Renilla luciferase cDNA (Promega) in a final volume of 0.2 mL, using Lipofectamine 2000 (Invitrogen) for 48 h. After that, protein was extracted from these fibroblasts and subjected to measurement of Firefly and Renilla luciferase activities using the Dual Glo Luciferase assay kit (Promega).

*Protein array analysis*

The treated fibroblasts samples were harvested and sent to Raybiotech (Norcross, GA, USA) in dry ice for protein array analysis. The concentration of each protein sample was adjusted to 500 μg/mL or 1000 μg/mL and then subjected to the analysis of differentially expressed proteins using the 487-protein Quantibody array (PAH-G2, Raybiotech), which is composed of antibody coated onto a glass slide for the detection of cytokines, chemokines, soluble receptor, and growth factors. Each protein sample was diluted on a standard curve with a purified standard protein. Each array contained positive control and was used for normalization. The fluorescent intensity of the bound labeled antibodies to each spot (protein or peptide) was measured in triplicate spots and averaged for data analysis and normalization using

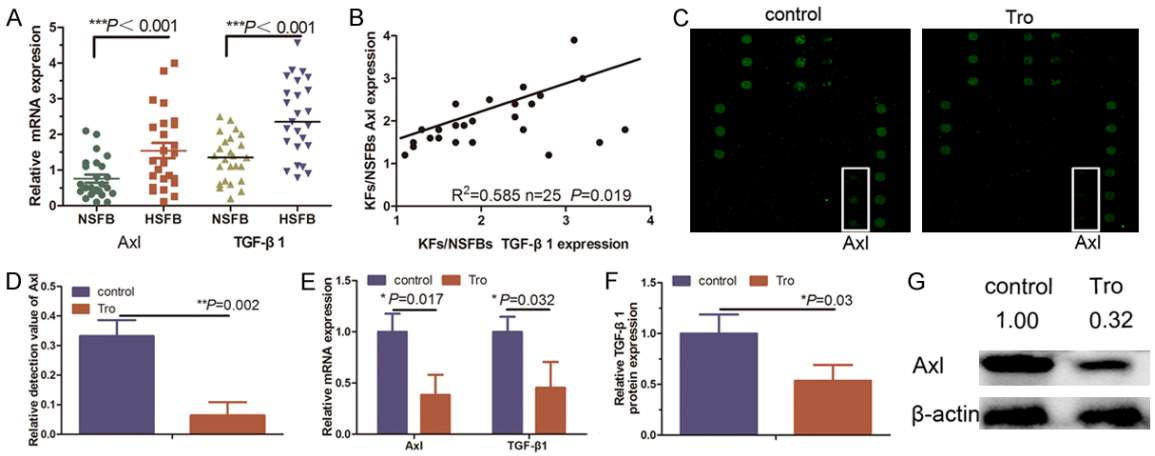


**Figure 1.** Troglitazone inhibition of upregulated TGF-β1 and Axl expression in KFs. (A) qRT-PCR. KFs and NSFBs were isolated from 25 keloid patients and healthy controls and then 3 passages of cells were subjected to qRT-PCR analysis. The data showed upregulated expression of both (***$P < 0.001$). (B) Association of TGF-β1 with Axl levels in KFs/NSFBs (*$P = 0.019$). (C) Protein array analysis. KFs with or without treatment with troglitazone were subjected to the protein array analysis. Rectangles indicate Axl. (D) Quantification of Axl level in KFs treated with or without troglitazone in (C). Data are expressed as mean ± SD (**$P = 0.002$). (E) qRT-PCR. Levels of TGF-β1 mRNA in KFs treated with or without troglitazone were assessed using qRT-PCR (*$P = 0.017$ and *$P = 0.032$). The data were summarized as mean ± SD of three independent experiments. (F) ELISA. Levels of TGF-β1 protein in KFs-cultured media after troglitazone treatment were assessed using ELISA (*$P = 0.03$). Experiments were in duplicate and repeated three times and the data are expressed as means ± SD. (G) Western blot. The duplicated cells were subjected to Western blot analysis and quantified with Image J software after normalization to β-actin.

Raybiotech software. The data are expressed and reported as pg of protein/mL extract.

*Enzyme-linked immunosorbent assay (ELISA)*

Fibroblast culture media, after various treatments or gene transfections, were collected for ELISA detection of TGF-β1 level using a TGF-β1 kit from eBioscience Inc. (San Diego, CA, USA) according to the manufacturer's instructions. The TGF-β1 ELISA 96-well plates were first briefly incubated with the wash buffer and 100 μL conditioned cell culture medium of each treatment was added to 96-well plates in triplicate and incubated at 4°C overnight, then washed with the wash buffer and a secondary avidin-horseradish peroxidase-conjugated antibody was added from the kit and incubated at room temperature for 30 min. After being washed with the wash buffer, the plates were subjected to color reaction using tetramethylbanzedine substrate; optical density (OD) values were measured using Nano Drop 2000 (Thermo Fisher Scientific, Inc., Waltham, MA, USA) at 450 nm.

*Chromatin immunoprecipitation (ChIP)*

The ChIP assay was performed with the Magna ChIP A/G kit (Millipore, Billerica, MA, USA), according to the manufacturer's protocol. Briefly, KFs were grown to reach approximately 95% confluency in 100 mm cell culture dishes and treated with troglitazone. At the end of the treatment, cell culture was added with 16% methanol-free formaldehyde (Fisher Scientific, Waltham, MA, USA), to make a final concentration of 1%. Cross-linked cells were collected in ice-cold PBS and sonicated six times for 15 s pulses at 50 s intervals to reduce the size of the genomic DNA to 200-1000 bp. Then the sheared chromatin and magnetic beads were immunoprecipitated with anti-PPAR-γ (ab45-036, Abcam) or normal rabbit IgG overnight at 4°C on a rotator. The resulting magnetic bead-antibody-chromatin complex was washed once with a low-salt buffer, followed by high salt, LiCl, and TE buffers. The chromatin complex was then eluted and incubated at 62°C for 2 h. The DNA samples were recovered using spin columns and amplified using qPCR with primers of 5'-GCCGTTATGTACTTAAGAGGCAG-3' and 5'-CAGCCTCCTGAGTAGCTGGGGT-3'.

*Bioinformatic analysis*

miR-92b non-redundant targets were predicted using the miRNA target prediction tools (Targetminer, www.isical.ac.in/bioinfo_miu and Tarbase, http://microrna.gr/tarbase/). These

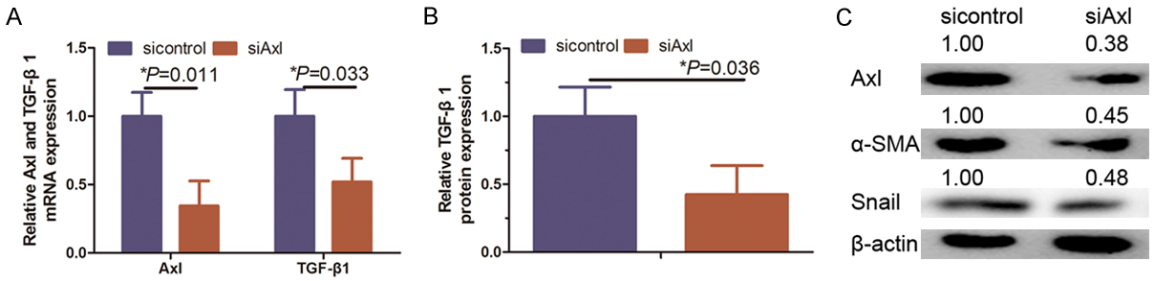


**Figure 2.** Effect of Axl knockdown on regulation of TGF-β1 and pathway genes. A: qRT-PCR. KFs were grown and transfected with Axl siRNA1 and then subjected to qRT-PCR analysis. The experiments were repeated three times and the data are presented as means ± SD. **P* = 0.011 and ***P* = 0.033. B: ELISA. The culture media from A were subjected to ELISA. The experiments were repeated three times and the data are presented as means ± SD. **P* = 0.036. C: Western blot. KFs were grown and transfected with Axl siRNA and then subjected to Western blot analysis and quantified with Image J software after normalization to β-actin.

target genes were then mapped onto gene ontology (GO) terms with DAVID version 6.7 (http://david.abcc.ncifcrf.gov/) and analyzed.

*Statistical analysis*

All data were summarized as mean ± standard deviation (SD) of at least three independent experiments. The difference between groups was statistically analyzed using two-sided Student's *t*-tests; Correlation between the Axl and TGF-β1 expression was assessed by using Pearson's correlation test. $P < 0.05$ was considered statistically significant (*$P < 0.05$, **$P < 0.01$, and ***$P < 0.001$). All statistical analyses were performed using PRISM software, version 4 (GraphPad Software, La Jolla, CA, USA).

## Results

*Elevation of TGF-β1 and Axl proteins in fibroblasts obtained from keloid patients vs. healthy controls*

We first analyzed the levels of TGF-β1 and Axl mRNA in fibroblasts from keloid patients and healthy controls (n = 25 of each), finding that TGF-β1 and Axl levels were statistically significantly elevated in keloid patients (**Figure 1A**). We also found that levels of endogenous Axl expression were associated with levels of TGF-β1 mRNA (**Figure 1B**). These data indicate that TGF-β and Axl could be involved in collagen synthesis and a functional link between Axl and TGF-β1 in keloids.

Thus, we then assessed whether PPAR-γ agonist troglitazone can regulate TGF-β and signaling by treating KFs with 30 mM troglitazone for 72 h, the dose of which was according to our previous study [23]. Our protein array analysis showed that Axl was indeed downregulated for more than 6 folds after troglitazone treatment (**Figure 1C** and **1D**). Our qRT-PCR, ELISA, and Western blot data also showed that levels of TGF-β1 mRNA and protein were significantly reduced (**Figure 1E** and **1F**), while Axl was at least 3-folds downregulated compared to the controls (**Figure 1E** and **1G**).

*Effect of Axl knockdown on inhibition of TGF-β1 and pathway in KFs*

Next, we knocked down Axl expression using Axl siRNA according to a previous study [25, 26] showing that Axl upregulated expression of TGF-β1 and TGF-β1 downstream effectors in KFs. As shown in **Figure 2**, Axl siRNA was able to significantly reduce Axl expression at both the mRNA and protein levels (**Figure 2A** and **2B**), which also resulted in reduction of the expression of TGF-β1 and its pathway genes, like α-SMA and Snail in KFs or culture media (**Figure 2C**).

*Effect of troglitazone on inhibition of Axl expression through upregulation of miR-92b in KFs*

Then we analyzed Axl gene promoter to assess whether it contains PPRE, but we failed. Thus, we thought miRNAs may play a role in bridging troglitazone in regulated Axl expression. Indeed, our previous microarray data showed that PPAR-γ agonist induced expression of miR-92b in KFs.

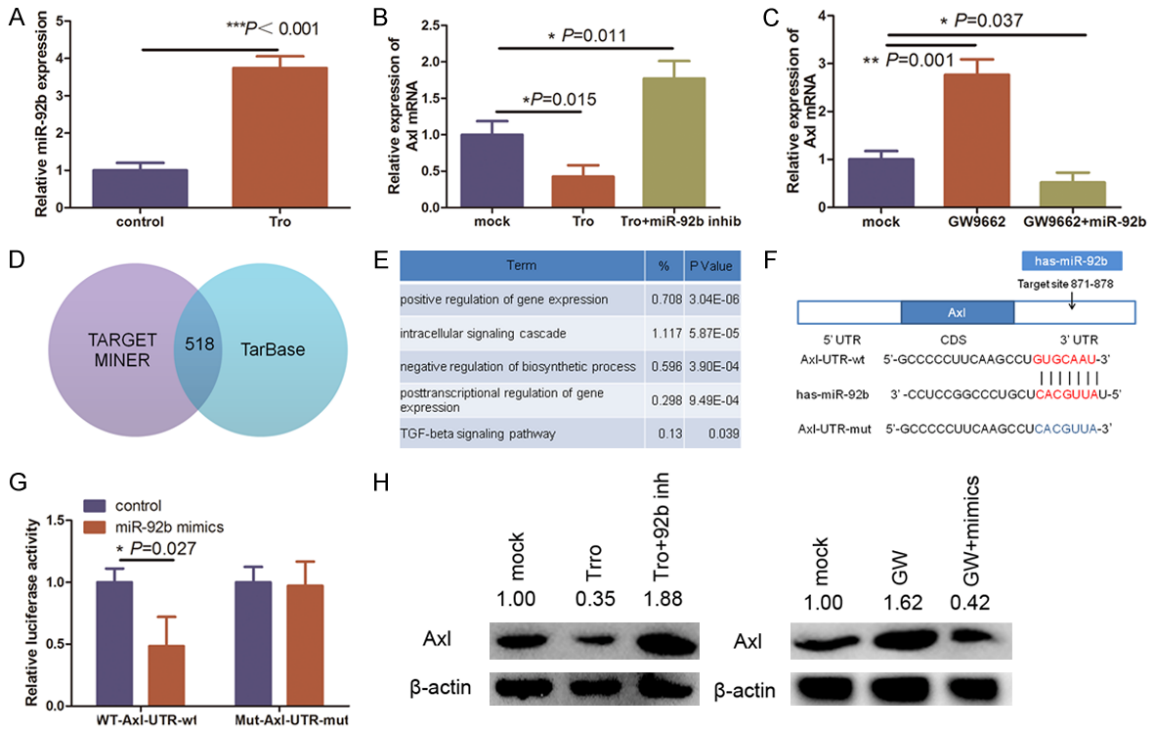


**Figure 3.** Effect of troglitazone-upregulated miR-92b on inhibition of Axl expression in KFs. (A) qRT-PCR. Levels of miR-92b in KFs treated with troglitazone (Tro) was analyzed using qRT-PCR. ***$P < 0.001$. (B) qRT-PCR. Levels of Axl in KFs treated with Tro or Tro plus miR-92b inhibitor were analyzed using qRT-PCR. *$P = 0.011$ and **$P = 0.015$. (C) qRT-PCR. Levels of Axl in KFs treated with GW9662 or GW9662 plus miR-92b mimics were analyzed using qRT-PCR. *$P = 0.037$ and **$P = 0.001$. (D) The Go classification of miR-92b potential targets using Targetminer and Tarbase algorithms. (E) Pathway enrichment analysis of 518 genes from (D). (F) Bioinformatic analysis. Putative miR-92b-binding site in Axl 3'-UTR. Mutation was generated on the Axl 3'-UTR site. (G) Luciferase activity. KFs were co-transfected with a control renilla luciferase expression construct pRL-TK, firefly luciferase reporter plasmid containing either wild-type or mutant Axl 3'-UTR, and miR-92b mimics or control for 48 h and then subjected to luciferase activity assay. Firefly luciferase activity of each sample was normalized by Renilla luciferase activity. The normalized luciferase activity for the scramble-transfected cells was set as relative luciferase activity. The columns showed the mean of at least three independent experiments in duplicate. *$P = 0.027$. (H) Western blot. KFs with corresponding treatment were subjected to the assay. Tro, troglitazone; Tro plus miR-92b, Tro + miR-92b inhibitor; GW, GW9662 or GW9662 plus miR-92b mimics.

We first confirmed these data, finding that PPAR-γ agonist treatment of KFs did induce miR-92b expression (**Figure 3A**). Moreover, we evaluated miR-92b in the regulation of Axl expression by the knockdown of miR-92b using a miR-92b specific inhibitor on troglitazone treatment for 72 h or by overexpression of miR-92b using miR-92b mimics on GW9662 treatment for 48 h. As shown in **Figure 3B**, troglitazone markedly reduced level of Axl mRNA, whereas the addition of miR-92b inhibitor restored the level of Axl mRNA. In contrast, GW9662 completely reversed the inhibitory effects of miR-92b mimics on Axl expression (**Figure 3C**).

We performed a computer-aided algorithmic analysis using Targetminer and Tarbase, finding that miR-92b was able to target 518 genes in the human genome (**Figure 3D**). The GO analysis of miR-92b targeting genes showed that these targeting genes function in several important cell processes, including TGF-β signaling pathway (**Figure 3E**) and that Axl was identified as a potential target gene of miR-92b, further confirming our experimental data (**Figure 3C**). Then we cloned the 3'-UTR of Axl cDNA, which may have contained the potential miR-92b binding site, and performed luciferase reporter assay. Our data showed that, compared to the scramble control, the miR-92b mimics significantly decreased relative luciferase activity in co-transfection with the Axl 3'-UTR reporter plasmid (**Figure 3F** and **3G**). However, the mutant reporter plasmid abolished this effect of the miR-92b mimics (**Figure 3G**). Furthermore,

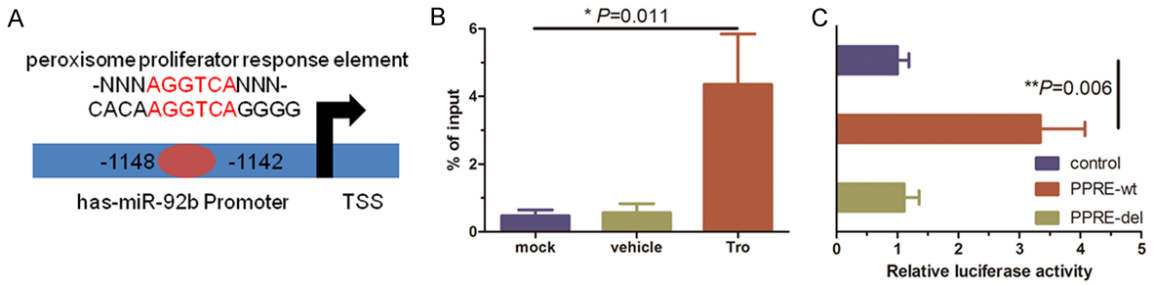


**Figure 4.** Activation of miR-92b transcription trough PPAR-γ binding to miR-92b promoter. A: Schematic illustration of miR-92b promoter upstream constructs. It contains a putative PPRE binding site. B: ChIP-qPCR analysis. KFs were treated with troglitazone and protein-DNA complex was extracted for ChIP assay. The resulted DNA samples were subjected to qPCR amplification of the PPRE in miR-92b promoter regions. Error bars, mean ± SD of three repeated experiments. *$P$ = 0.011. C: Luciferase activity assay. Luciferase activity data showed PPAR-γ binding to miR-92b wild type but not mutated promoter. The data are expressed as mean ± SD of three independent experiments. **$P$ = 0.006.

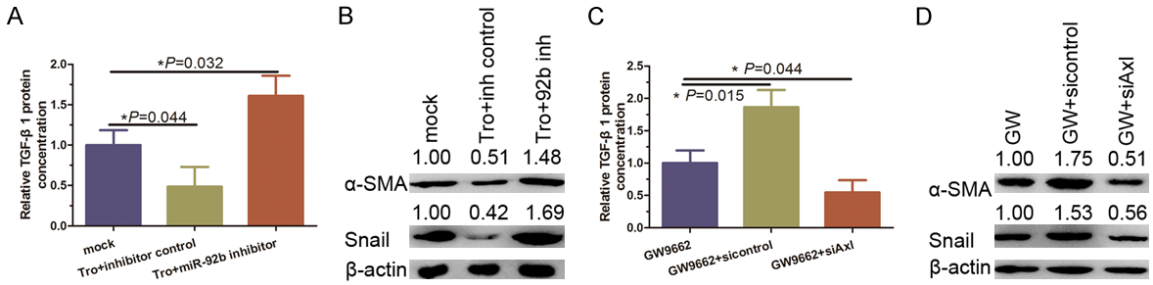


**Figure 5.** Effect of troglitazone-upregulated miR-92b on regulation of TGF-β1 and signaling proteins in KFs. A: ELISA. KFs were treated with troglitazone plus negative control inhibitor or miR-92b inhibitor for 48 h and the cell cultured conditioned medium was subjected to ELISA analysis of TGF-β1 level. *$P$ = 0.044 and **$P$ = 0.032. B: Western blot. Levels of TGF-β pathway protein α-SMA and Snail (mean ± SD) in KFs after treatment with troglitazone plus negative control inhibitor or miR-92b inhibitor were subjected to Western blot. C: ELISA. The secreted TGF-β1 levels were assessed using ELISA in KFs after 48 h treatment with GW9662, GW9662 + sicontrol and GW9662 + siAxl. *$P$ = 0.015 and **$P$ = 0.044. D: Western blot. The TGF-β pathway protein α-SMA and Snail protein levels in KFs after treatment with GW9662, GW9662 + sicontrol and GW9662 + siAxl were analyzed using Western blot.

Western blot data showed that transfection of miR-92b inhibitor not only abolished the effects of PPAR-γ agonist, but also further induced Axl expression (**Figure 3H**), whereas transfection of miR-92b mimics had the inverse effects (**Figure 3H**). This finding further confirmed that miR-92b mediated the effect of troglitazone on the inhibition of Axl expression in KFs.

*PPAR-γ transcriptional regulation of miR-92b expression*

Then we analyzed miR-92b gene promoter for PPRE sites, finding a potential one; thus, we cloned a 2 kb DNA fragment corresponding to the promoter region onto a luciferase reporter plasmid and generated a mutated PPRE plasmid PPRE-del (**Figure 4A**). Our luciferase assay data showed that the transcriptional activity of the plasmid carrying the wild type promoter was upregulated after troglitazone treatment, whereas the mutated plasmid did not have such an effect (**Figure 4B**). Our ChIP-PCR assay data further confirmed that troglitazone-activated PPAR-γ bound to the potential PPRE site in the miR-92b promoter region (**Figure 4C**). These data demonstrate that miR-92b is a novel PPAR-γ transcriptional target.

*Effects of miR-92b on inhibition of Axl and TGF-β pathway*

To assess whether aberrant miR-92b expression could alter TGF-β signaling in KFs, we disrupted miR-92b and Axl expression. Our data showed that transfection of miR-92b inhibitor suppressed the effects of PPAR-γ agonist on inhibition of TGF-β1 and TGF-β pathway (**Figure**

**5A** and **5B**). Moreover, Axl siRNA also abolished the effects of PPAR-γ antagonist on induced expression of TGF-β1 and TGF-β pathway proteins (**Figure 5C** and **5D**).

## Discussion

PPAR-γ agonist has shown a role in prevention and treatment of skin fibrosis and the underlying mechanisms were not fully understood [27]. In the current study, we explored and demonstrated that PPAR-γ agonist is a TGF-β pathway repressor. Particularly, we found that levels of TGF-β1 and Axl proteins were significantly higher in 25 cases of KFs than in NSFBs and that troglitazone treatment significantly reduced levels of TGF-β1 and Axl in KFs. Knockdown of Axl expression downregulated expression of TGF-β1 and its pathway genes. PPAR-γ does not directly decrease Axl expression, but acts through the transcriptional activation of miR-92b, as confirmed by luciferase and ChIP-PCR assays, showing that miR-92b promoter contains PPRE sequences. miR-92b mimics inhibited Axl expression at both mRNA and protein levels, whereas GW9662 completely reversed the inhibitory effects of miR-92b mimics on Axl expression in KFs. The GO analysis of miR-92b targeting genes and luciferase assay predicted and confirmed that Axl was indeed a miR-92b target gene. Our current data demonstrated that PPAR-γ-induced miR-92b expression suppressed Axl expression to in turn reduce expression of TGF-β1 and downstream genes in KFs as the molecular mechanism of troglitazone action in KFs. Pending on further confirmation using *in vivo* data, our current study suggests that the manipulation of this gene pathway could be a novel strategy in control of fibrosis or keloid in clinic.

Axl belongs to the receptor tyrosine kinase subfamily, and the Axl protein possesses a unique structure for the extracellular region, which gives it an ability to transduce extracellular matrix signals into the cytoplasm and stimulate cell proliferation [28]; thus, upregulated Axl expression has been shown to be associated with the development of various types of human cancer: Axl may be a therapeutic target in control of human cancers [29]. To date, controversial data have also been shown in the literature. For example, Bauer *et al*. reported that TGF-β1-induced Axl enhanced apoptosis and blocked proinflammatory cytokine production, suggesting that Axl was a downstream effector of TGF-β1 during Langerhans cell differentiation and epidermal homeostasis [30], whereas Li *et al*. showed that Axl was a downstream effector of TGF-β1 for the promotion of breast cancer invasion and chemoresistance [31]. Calvisi *et al*. found that Axl activated TGF-β target genes, such as Snail in hepatocellular carcinoma cells [32]. In our current study, we found that both TGF-β1 and Axl were upregulated in KFs from 25 keloid patients compared to NSFBs. Troglitazone treatment significantly reduced levels of TGF-β1 and Axl proteins in KFs. Moreover, knockdown of Axl expression using Axl siRNA downregulated expression of TGF-β1 and its pathway genes, which supports the data in a previous study [30]. Our current data also support previous studies that showed troglitazone had a rapid anti-fibrosis effect in animal models and *in vitro* experiments by targeting of the anti-TGF-β pathway [18, 33-35] and that levels of the pro-fibrosis TGF-β and pathway genes were increased in keloids or KFs [36-39]. However, our analysis did not find PPRE sites in Axl gene promoter (data not shown), which led us to relate miRNAs to the gene regulation picture.

miRNAs are a class of endogenous small noncoding RNAs that posttranscriptionally regulate expression of target genes [40, 41]. A mature miRNA is of approximately 18-22 nucleotides in length [40] and imperfectly complementarily binds to the 3'-untranslated region (3'-UTR) of the targeted gene to degrade mRNA or inhibit mRNA translation [41]. Thus, miRNAs play an important role in regulation of cell proliferation, apoptosis, and differentiation; in the skin, miRNAs may relate to the etiology and progression of fibrotic diseases [42, 43]. Our previous study showed that upregulated miR-145 participated in feedback regulation, involving in PPAR-γ agonist and antagonist-modulated collagen synthesis in hypertrophic scar fibroblasts [24]. The change in specific miRNA expression profiles can have a dramatic effect on fibrosis, suggesting that modulating miRNA expression may be a novel approach for developing innovative therapeutic strategies [43]. Our current data showed that troglitazone-activated PPAR-γ could bind to miR-92b promoter to induced miR-92b expression in KFs, which in turn downregulates Axl expression and then TGF-β1 levels in KFs. Indeed, our previous study of miRNAs in glioma cells demonstrated that knock-

down of miR-92b expression significantly reduced glioma cell viability through upregulation of the TGF-β/Smad3/p21 signaling pathway *in vitro* [44]; our current study further supports Axl-repressing TGF-β1 in different types of cells. Furthermore, miR-92b has a oncogene role in many types of human cancer by promoting cancer cell growth and chemoresistance to cisplatin [45, 46].

However, our current study has only explored the underlying molecular events of troglitazone anti-fibrosis activity in KFs *in vitro*: further investigation is needed to: confirm our current study using an animal model to assess the effect of troglitazone-activated PPAR-γ on regulation of TGF-β1 expression in KFs, or confirm the PPAR-γ-led miR-92b in inhibition of Axl and TGF-β1 expression in suppression of keloid formation *in vivo*. In conclusion, our current study demonstrated that the effect of PPAR-γ agonist troglitazone-suppressed fibrosis during keloid formation was through troglitazone-induced miR-92b expression to in turn inhibit expression of Axl and TGF-β1 in KFs. Our current data suggest that troglitazone treatment and even modulation of this gene pathway could be useful for control of fibrosis or keloid in clinic.

## Acknowledgements

This study was supported in part by grants from National Natural Science Foundation of China (81372069, 81171811, 81571914, 81501-684, and 81201470) and Natural Science Foundation of Shaanxi Province (2015JM8453).

## Disclosure of conflict of interest

None.

**Address correspondence to:** Da-Hai Hu and Song-Tao Xie, Department of Burns and Cutaneous Surgery, Xijing Hospital, Fourth Military Medical University, 127 Changle Xilu, Xi'an 710032, Shaanxi, China. Tel: 862984775298; E-mail: zzhuhy@aliyun.com (DHH); burnskeloid@qq.com (STX)

## References

[1] Kashiyama K, Mitsutake N, Matsuse M, Ogi T, Saenko VA, Ujifuku K, Utani A, Hirano A, Yamashita S. miR-196a downregulation increases the expression of type I and III collagens in keloid fibroblasts. J Invest Dermatol 2012; 132: 1597-1604.

[2] Vincent AS, Phan TT, Mukhopadhyay A, Lim HY, Halliwell B, Wong KP. Human skin keloid fibroblasts display bioenergetics of cancer cells. J Invest Dermatol 2008; 128: 702-709.

[3] Zhao Y, Liu SL, Xie J, Ding MQ, Lu MZ, Zhang LF, Yao XH, Hu B, Lu WS, Zheng XD. NEDD4 single nucleotide polymorphism rs2271289 is associated with keloids in Chinese Han population. Am J Transl Res 2016; 8: 544-555.

[4] Xue D, Qian H. Surgical management for large chest keloids with internal mammary artery perforator flap. An Bras Dermatol 2016; 91: 103-105.

[5] Abbas A, Blandon J, Rude J, Elfar A, Mukherjee D. PPAR-γ agonist in treatment of diabetes: cardiovascular safety considerations. Cardiovasc Hematol Agents Med Chem 2012; 10: 124-134.

[6] Lu G, Zhang G, Zheng X, Zeng Y, Xu Z, Zeng W, Wang K. c9, t11- conjugated linoleic acid induces HCC cell apoptosis and correlation with PPAR-γ signaling pathway. Am J Transl Res 2015; 7: 2752-2763.

[7] Belfiore A, Genua M, Malaguarnera R. PPAR-gamma agonists and their effects on IGF-I receptor signaling: Implications for cancer. PPAR Res 2009; 2009: 830501.

[8] Ferroni P, Della-Morte D, Pileggi A, Riondino S, Rundek T, Ricordi C, Guadagni F. Pleiotropic effects of PPARγ agonist on hemostatic activation in type 2 diabetes mellitus. Curr Vasc Pharmacol 2013; 11: 338-351.

[9] Yan S, Yang X, Chen T, Xi Z, Jiang X. The PPARγ agonist Troglitazone induces autophagy, apoptosis and necroptosis in bladder cancer cells. Cancer Gene Ther 2014; 21: 188-193.

[10] Cao LQ, Shao ZL, Liang HH, Zhang DW, Yang XW, Jiang XF, Xue P. Activation of peroxisome proliferator-activated receptor-γ (PPARγ) inhibits hepatoma cell growth via downregulation of SEPT2 expression. Cancer Lett 2015; 359: 127-135.

[11] Smallridge RC, Copland JA, Brose MS, Wadsworth JT, Houvras Y, Menefee ME, Bible KC, Shah MH, Gramza AW, Klopper JP, Marlow LA, Heckman MG, Von Roemeling R. Efatutazone, an oral PPAR-γ agonist, in combination with paclitaxel in anaplastic thyroid cancer: results of a multicenter phase 1 trial. J Clin Endocrinol Metab 2013; 98: 2392-2400.

[12] Komatsu Y, Yoshino T, Yamazaki K, Yuki S, Machida N, Sasaki T, Hyodo I, Yachi Y, Onuma H, Ohtsu A. Phase 1 study of efatutazone, a novel oral peroxisome proliferator-activated receptor gamma agonist, in combination with FOLFIRI as second-line therapy in patients with metastatic colorectal cancer. Invest New Drugs 2014; 32: 473-480.

[13] Small DM, Morais C, Coombes JS, Bennett NC, Johnson DW, Gobe GC. Oxidative stress-induced changes in PPAR-γ and associated mitochondrial destabilization contribute to kidney cell apoptosis. Am J Physiol Renal Physiol 2014; 307: F814-822.
[14] Liu L, Yang Z, Xu Y, Li J, Xu D, Zhang L, Sun J, Xia S, Zou F, Liu Y. Inhibition of oxidative stress-elicited AKT activation facilitates PPARγ agonist-mediated inhibition of stem cell character and tumor growth of liver cancer cells. PLoS One 2013; 8: e73038.
[15] Xu P, Lou XL, Chen C, Yang ZW. Effects of peroxisome proliferator-activated receptor-γ activation on apoptosis in rats with acute pancreatitis. Dig Dis Sci 2013; 58: 3516-3523.
[16] Mangoni M, Sottili M, Gerini C, Bonomo P, Bottoncetti A, Castiglione F, Franzese C, Cassani S, Greto D, Masoni T, Meattini I, Pallotta S, Passeri A, Pupi A, Vanzi E, Biti G, Livi L. A PPAR-gamma agonist attenuates pulmonary injury induced by irradiation in a murine model. Lung Cancer 2015; 90: 405-409.
[17] Zhang GY, Yi CG, Li X, Ma B, Li ZJ, Chen XL, Guo SZ, Gao WY. Troglitazone suppresses transforming growth factor-β1-induced collagen type I expression in keloid fibroblasts. Br J Dermatol 2009; 160: 762-770.
[18] Malaguarnera M, Motta M, Vacante M, Malaguarnera G, Caraci F, Nunnari G, Gagliano C, Greco C, Chisari G, Drago F, Bertino G. Silybin-vitamin E-phospholipids complex reduces liver fibrosis in patients with chronic hepatitis C treated with pegylated interferon α and ribavirin. Am J Transl Res 2015; 7: 2510-2518.
[19] Ha DM, Carpenter LC, Koutakis P, Swanson SA, Zhu Z, Hanna M, De Spiegelaere HK, Pipinos II, Casale GP. Transforming growth factor-beta 1 produced by vascular smooth muscle cells predicts fibrosis in the gastrocnemius of patients with peripheral artery disease. J Transl Med 2016; 14: 39.
[20] Lichtman MK, Otero-Vinas M, Falanga V. Transforming Growth Factors β (TGF-β) Isoforms in Wound Healing and Fibrosis. Wound Repair Regen 2016; 24: 215-222.
[21] Lin L, Wang Y, Liu W, Huang Y. BAMBI inhibits skin fibrosis in keloid through suppressing TGF-β1-induced hypernomic fibroblast cell proliferation and excessive accumulation of collagen I. Int J Clin Exp Med 2015; 8: 13227-13234.
[22] Zhang GY, Cheng T, Zheng MH, Yi CG, Pan H, Li ZJ, Chen XL, Yu Q, Jiang LF, Zhou FY, Li XY, Yang JQ, Chu TG, Gao WY. Peroxisome proliferator-activated receptor-gamma (PPAR-gamma) agonist inhibits transforming growth factor-beta1 and matrix production in human dermal fibroblasts. J Plast Reconstr Aesthet Surg 2010; 63: 1209-1216.
[23] Zhu HY, Li C, Zheng Z, Zhou Q, Guan H, Su LL, Han JT, Zhu XX, Wang SY, Li J, Hu DH. Peroxisome proliferator-activated receptor-γ (PPAR-γ) agonist inhibits collagen synthesis in human hypertrophic scar fibroblasts by targeting Smad3 *via* miR-145. Biochem Biophys Res Commun 2015; 459: 49-53.
[24] Escher P, Wahli W. Peroxisome proliferator-activated receptors: insight into multiple cellular functions. Mutat Res 2000; 448: 121-138.
[25] Reichl P, Dengler M, van Zijl F, Huber H, Führlinger G, Reichel C, Sieghart W, Peck-Radosavljevic M, Grubinger M, Mikulits W. Axl activates autocrine transforming growth factor-β signaling in hepatocellular carcinoma. Hepatology 2015; 61: 930-941.
[26] Wei J, Zhu H, Komura K, Lord G, Tomcik M, Wang W, Doniparthi S, Tamaki Z, Hinchcliff M, Distler JH, Varga J. A synthetic PPAR-γ agonist triterpenoid ameliorates experimental fibrosis: PPAR-γ-independent suppression of fibrotic responses. Ann Rheum Dis 2014; 73: 446-454.
[27] Lakota K, Wei J, Carns M, Hinchcliff M, Lee J, Whitfield ML, Sodin-Semrl S, Varga J. Levels of adiponectin, a marker for PPAR-gamma activity, correlate with skin fibrosis in systemic sclerosis: potential utility as biomarker? Arthritis Res Ther 2012; 14: R102.
[28] Janssen JW, Schulz AS, Steenvoorden AC, Schmidberger M, Strehl S, Ambros PF, Bartram CR. A novel putative tyrosine kinase receptor with oncogenic potential. Oncogene 1991; 6: 2113-2120.
[29] Wu X, Liu X, Koul S, Lee CY, Zhang Z, Halmos B. AXL kinase as a novel target for cancer therapy. Oncotarget 2014; 5: 9546-9563.
[30] Bauer T, Zagórska A, Jurkin J, Yasmin N, Köffel R, Richter S, Gesslbauer B, Lemke G, Strobl H. Identification of Axl as a downstream effector of TGF-β1 during Langerhans cell differentiation and epidermal homeostasis. J Exp Med 2012; 209: 2033-2047.
[31] Li Y, Jia L, Liu C, Gong Y, Ren D, Wang N, Zhang X, Zhao Y. Axl as a downstream effector of TGF-β1 via PI3K/Akt-PAK1 signaling pathway promotes tumor invasion and chemoresistance in breast carcinoma. Tumour Biol 2015; 36: 1115-1127.
[32] Calvisi DF. When good transforming growth factor-β turns bad in hepatocellular carcinoma: Axl takes the stage. Hepatology 2015; 61: 759-761.
[33] van Westerloo DJ, Florquin S, de Boer AM, Daalhuisen J, de Vos AF, Bruno MJ, van der Poll T. Therapeutic effects of troglitazone in experimental chronic pancreatitis in mice. Am J Pathol 2005; 166: 721-728.

[34] Kawai T, Masaki T, Doi S, Arakawa T, Yokoyama Y, Doi T, Kohno N, Yorioka N. PPAR-gamma agonist attenuates renal interstitial fibrosis and inflammation through reduction of TGF-beta. Lab Invest 2009; 89: 47-58.

[35] Marra F, DeFranco R, Robino G, Novo E, Efsen E, Pastacaldi S, Zamara E, Vercelli A, Lottini B, Spirli C, Strazzabosco M, Pinzani M, Parola M. Thiazolidinedione treatment inhibits bile duct proliferation and fibrosis in a rat model of chronic cholestasis. World J Gastroenterol 2005; 11: 4931-4938.

[36] Lee TY, Chin GS, Kim WJ, Chau D, Gittes GK, Longaker MT. Expression of transforming growth factor beta 1, 2, and 3 proteins in keloids. Ann Plast Surg 1999; 43: 179-184.

[37] Zhou P, Shi L, Li Q, Lu D. Overexpression of RACK1 inhibits collagen synthesis in keloid fibroblasts via inhibition of transforming growth factor-β1/Smad signaling pathway. Int J Clin Exp Med 201; 8: 15262-15268.

[38] Hsu YC, Hsiao M, Chien YW, Lee WR. Exogenous nitric oxide stimulated collagen type I expression and TGF-beta1 production in keloidfibroblasts by a cGMP-dependent manner. Nitric Oxide 2007; 16: 258-265.

[39] Hanasono MM, Kita M, Mikulec AA, Lonergan D, Koch RJ. Autocrine growth factor production by fetal, keloid, and normal dermal fibroblasts. Arch Facial Plast Surg 2003; 5: 26-30.

[40] Ma J, Shui S, Han X, Guo D, Li T, Yan L. microRNA-22 attenuates neuronal cell apoptosis in a cell model of traumatic brain injury. Am J Transl Res 2016; 8: 1895-1902.

[41] Geng Z, Xu F, Zhang Y. MiR-129-5p-mediated Beclin-1 suppression inhibits endothelial cell autophagy in atherosclerosis. Am J Transl Res 2016; 8: 1886-1894.

[42] Miller KJ, Brown DA, Ibrahim MM, Ramchal TD, Levinson H. MicroRNAs in skin tissue engineering. Adv Drug Deliv Rev 2015; 88: 16-36.

[43] Song L, Shi S, Jiang W, Liu X, He Y. Protective role of propofol on the kidney during early unilateral ureteral obstruction through inhibition of epithelial-mesenchymal transition. Am J Transl Res 2016; 8: 460-472.

[44] Wu ZB, Cai L, Lin SJ, Lu JL, Yao Y, Zhou LF. The miR-92b functions as a potential oncogene by targeting on Smad3 in glioblastomas. Brain Res 2013; 1529: 16-25.

[45] Lei L, Huang Y, Gong W. Inhibition of miR-92b suppresses nonsmall cell lung cancer cells growth and motility by targeting RECK. Mol Cell Biochem 2014; 387: 171-176.

[46] Haug BH, Henriksen JR, Buechner J, Geerts D, Tømte E, Kogner P, Martinsson T, Flægstad T, Sveinbjørnsson B, Einvik C. MYCN-regulated miRNA-92 inhibits secretion of the tumor suppressor DICKKOPF-3 (DKK3) in neuroblastoma. Carcinogenesis 2011; 32: 1005-1012.